Activity of the RhoU/Wrch1 GTPase is critical for cranial neural crest cell migration

Philippe Fort [a,b,*], Linda Guémar [a,b], Emmanuel Vignal [a,b], Nathalie Morin [a,b], Cécile Notarnicola [c], Pascal de Santa Barbara [c], Sandrine Faure [a,b,c,*,1]

[a] Universités Montpellier 2 et 1, CRBM, IFR122, Montpellier, France
[b] CNRS UMR 5237, 1919 Route de Mende, 34293 Montpellier, France
[c] INSERM, ERI 25 EA 4202, 34295 Montpellier, France

ARTICLE INFO

Keywords:
Rho GTPases
RhoU
Cranial neural crest
Migration
Xenopus

ABSTRACT

The neural crest (NC) is a stem cell-like population that arises at the border of neural and non-neural ectoderm. During development, NC undergoes an epithelio-mesenchymal transition (EMT), i.e. loss of epithelial junctions and acquisition of pro-migratory properties, invades the entire embryo and differentiates into a wide diversity of terminal tissues. We have studied the implication of Rho pathways in NC development and previously showed that RhoV is required for cranial neural crest (CNC) cell specification. We show here that the non-canonical Wnt response *rhoU/wrch1* gene, closely related to *rhoV*, is also expressed in CNC cells but at later stages. Using both gain- and loss-of-function experiments, we demonstrate that the level of RhoU expression is critical for CNC cell migration and subsequent differentiation into craniofacial cartilages. In *in vitro* cultures, RhoU activates pathways that cooperate with PAK1 and Rac1 in epithelial adhesion, cell spreading and directional cell migration. These data support the conclusion that RhoU is an essential regulator of CNC cell migration.

Introduction

The Neural Crest (NC), an embryonic tissue unique to vertebrates, originates at the boundary between neural and non-neural ectoderm as the result of complex inductive signals (Huang and Saint-Jeannet, 2004), then migrates throughout the entire embryo and differentiates into many cell types, including neurons and glia of the peripheral nervous system, pigment cells and craniofacial bones and cartilages (Le Douarin and Dupin, 2003). Prior to migration, NC precursors undergo a delamination phase, characterized by the loss of epithelial adherens junctions and subsequent acquisition of migratory and invasive properties. This developmental process is reminiscent of early events of malignant progression, in which dysplasic epithelial adenoma cells switch to an invasive scattered carcinoma phenotype (Thiery et al., 2009). For these reasons, NC has attracted much attention in the past recent years for its stem cell-like and EMT properties.

NC induction at the neural plate border requires balanced levels of BMP, Wnt and FGF signals (Huang and Saint-Jeannet, 2004). As of Wnt signals, the current view in *Xenopus* is that the canonical β-catenin-dependent pathway is required for induction of NC specific genes, while the non-canonical pathway is involved in EMT, polarity, adhesion and migration (De Calisto et al., 2005; LaBonne and Bronner-Fraser, 1998; Matthews et al., 2008). Rho GTPases have recently emerged as key components of Wnt signaling, mostly involved in non-canonical pathways (Schlessinger et al., 2009). Cdc42, Rac1 and RhoA-B control several aspects of NC specification and migration stages (Broders-Bondon et al., 2007; Fuchs et al., 2009; Groysman et al., 2008; Liu and Jessell, 1998; Matthews et al., 2008). Rho GTPases are also involved in canonical Wnt signaling. Rac1 promotes JNK-dependent phosphorylation and nuclear accumulation of β-catenin (Wu et al., 2008) while RhoV/Chp, encoded in the *Xenopus* embryo by a canonical Wnt response gene, cooperates with Snai1/Snail for the transcriptional induction of *snai2/slug*, *sox9* or *twist* (Guemar et al., 2007). RhoV and RhoU/Wrch1 are two members of a distinct atypical Rho subclass that emerged in early multicellular organisms (Boureux et al., 2007). RhoU was initially identified as a non-canonical Wnt response gene (Tao et al., 2001). Unlike classical Rho members, RhoU exchanges GTP spontaneously (Saras et al., 2004; Shutes et al., 2006) and relies on palmitoylation for anchorage to membranes (Berzat et al., 2005). In cultured cells, RhoU activates Pak1 and JNK, elicits the formation of filopodia and focal adhesions, has a transforming activity on NIH3T3 cells and affects migration of different cell types (Chuang et al., 2007; Ory et al., 2007; Saras et al., 2004; Shutes et al., 2006; Tao et al., 2001).

Here, we explored the role of RhoU in embryonic *Xenopus* development and found that it is highly expressed in migrating CNC cells. Using both gain- and loss-of-function experiments, we provide evidence that the level of RhoU activity is critical for CNC cell

* Corresponding authors. Universités Montpellier 2 et 1, CRBM, IFR122, Montpellier, France. Fax: +33 4 67415231.
E-mail addresses: philippe.fort@crbm.cnrs.fr (P. Fort), sandrine.faure@inserm.fr (S. Faure).
[1] Present address.

directional migration *in vivo* and *in vitro*, likely by regulating cell adhesive properties.

Results

rhoU is expressed in migrating Xenopus CNC cells and is required for the migration process

We previously carried out an *in situ* hybridization (ISH) screen in *Xenopus* to identify Rho members essential for CNC cell differentiation and demonstrated that RhoV is critical for specification (Guemar et al., 2007). In the present paper, we focused on RhoU/Wrch1, the closest relative to RhoV/Chp. We first analyzed *rhoU* spatial expression pattern during *Xenopus* development by performing whole-mount ISH on a variety of embryonic stages (Fig. 1). *RhoU* transcripts were detected first at late gastrula stages (st. 12.5–st. 13) in the paraxial mesoderm and in two domains lateral to the neural plate (Fig. 1 panels A and B). Double *rhoU*/*sox9* ISH showed that the two *RhoU*-positive lateral domains are excluded from the *sox9* positive territory of the presumptive CNC (Fig. 1 panels C and D). During neurula stages (st. 14–st. 17), *rhoU* expression was found in the paraxial mesoderm and in otic placodes as shown by *rhoU*/*sox9* and *rhoU*/*twist* double ISH (Fig. 1 panels E–L). In contrast with *rhoV* (Guemar et al., 2007), *rhoU* was not detected in the CNC domain during specification. *RhoU* expression was found in migrating CNC cells, as demonstrated by *rhoU*/*twist* double ISH (Fig. 1 panels M–N), and maintained later on at tailbud stages in CNC cells migrating towards the branchial arches (Fig. 1 panels O–V). At these stages, *rhoU* was also strongly expressed in otic vesicles, eyes, the pronephric duct, tailbud, cement gland and in the anterior-most hatching glands.

To test whether *rhoU* is critical for NC development, we performed loss-of-function experiments using an anti-sense morpholino oligonucleotide (RhoU-MO) that we previously showed to block translation of a *RhoU-GFP* fusion mRNA, whereas it did not affect translation of a *RhoV-GFP* construct (Guemar et al., 2007). *Xenopus* embryos were co-injected in one cell of 4–8 cell stage with RhoU-MO and the nuclear beta-galactosidase (nβGal) mRNA as a lineage tracer. RhoU-MO-injected embryos cultured to the tadpole stage (stage 45) exhibited abnormal head morphology (Fig. 2A, compare panels a to c and panels b to d). Alcian blue stainings of the cranial cartilages revealed a reduction in size of the CNC-derived structures (Meckel's, branchial and cerathoyal cartilages) on the RhoU-MO injected side (Fig. 2A, compare panels f and g), indicating that RhoU is required for proper craniofacial development in *Xenopus* embryos. At earlier stages, no significant changes were observed in the expression of early CNC markers including *sox9*, *snail*, *slug* and *rhoV* (Spokony et al., 2002; Essex et al., 1993; Mayor et al., 1995; Guemar et al., 2007) (Supplemental Fig. 1A), thus ruling out a role for RhoU in specification. Last, RhoU activity was not critical for mesodermal development as indicated by the unchanged expression of *xbra* and *myoD* in RhoU knock-down embryos (Supplemental Fig. 1B).

RhoU is critical for CNC cell migration

To address whether RhoU is involved in CNC cell migration, we first injected one cell of 4–8 cell stage *Xenopus* embryos with RhoU-MO and nβGal mRNA as a lineage tracer. Injected embryos cultured to stage 22 were examined by ISH. As shown in Figs. 2B and C, CNC cell migrated laterally to populate the branchial arches in 97% (145/150) of uninjected control sides. By contrast, RhoU depletion induced dramatic effects on early CNC cell migration as visualized by expression of the *slug* and *twist* markers (Mayor et al., 1995; Hopwood et al., 1989). Only 29% (62/215) of RhoU-MO injected embryos exhibited normal migration compared to 91% (89/98) of embryos injected with control MO. These effects were not simply due to a delayed migration since staining of tailbud stage embryos for *sox9* and *twist*, which identify CNC cells in the three branchial arches (Spokony et al., 2002; Hopwood et al., 1989), confirmed the migration failure in MO-RhoU injected sides (Supplemental Fig. 1 C). Moreover, no significant changes in cell proliferation (assayed with phosphohistone H3 stainings) nor apoptotic cell death (monitored with TUNEL assays) were observed in MO-RhoU injected sides compared to control sides (data not shown). Hybridization of RhoU-MO injected embryos with the NC/hindbrain marker *krox-20* (Bradley et al., 1993) showed that RhoU knock-down inhibited migration of CNC cells from rhombomere 5 without affecting the hindbrain expression of this marker (Fig. 2B, panel d). When RhoU-MO was co-injected with a *GFP-Wt-RhoU* mRNA, insensitive to RhoU-MO, CNC cell migration was rescued (Fig. 2B, panel e), with 70% (85/122) of embryos exhibiting normal migration compared to 29% (62/215) with RhoU-MO alone (Figs. 2B and C). By contrast, expressed at the same amount as GFP-Wt-RhoU, GFP-Wt-RhoV was unable to rescue RhoU-MO depletion ($n=48$) (data not shown). Finally, we established that the migration defects observed in RhoU-MO morphants were CNC cell autonomous by performing transplantation experiments (Borchers et al., 2000). In these experiments, MO-treated CNC explants were isolated from fluorescently labeled embryos at the premigratory stage and transplanted into an unlabeled host embryo. At tailbud stages, grafted control-MO injected CNC cells migrated into the branchial arches in an organized manner whereas grafted RhoU-MO injected cells failed to reach the ventral edges of branchial arches (Fig. 2D). 93% (37/40) of grafted control MO embryos exhibited normal migration compared to 26% (11/42) of grafted RhoU-MO embryos (Figs. 2D, E). These results suggest that RhoU is required for CNC cell migration in *Xenopus*. To extend this observation to other vertebrates, we examined the requirement of RhoU in chick embryos, in which we previously showed *rhoU* expression in migrating CNC cells (Notarnicola et al., 2008). To this aim, we expressed GFP, alone or in combination with the dominant negative form of RhoU (T63N-RhoU) (Ory et al., 2007; Shutes et al., 2006) into the midbrain region of chick embryos at the 2–4 somite stage. Embryos were collected 8 h later and immunostained for HNK-1 to monitor possible changes in CNC cell migration (Fig. 3). Expression of GFP alone induced no changes in the appearance or in the number of migrating CNC cells ($n=6$) (Fig. 3 C). By contrast, co-expression of T63N-RhoU strongly impaired CNC cell emigration and migration in all embryos examined ($n=12$), as visualized by the absence of GFP/HNK-1 positive cells on the electroporated sides (Fig. 3F). These results indicate that the role of RhoU in CNC cell migration is conserved in frog and chick, and is therefore likely to be conserved in other vertebrates.

RhoU knock-down results in defect in cell attachment, spreading and migration in vitro

Our results indicate that RhoU is expressed in migrating CNC cells and is functionally required for the migration process. In order to understand the underlying mechanisms, we took advantage of an *in vitro* migratory system, in which cells from *Xenopus* CNC explants

Fig. 1. Localization of *rhoU* mRNA by ISH. ISH analysis of *rhoU* expression at different stages (st.) of development. (A, B, E, F), dorsal views. *rhoU* mRNA is detected at early neurula stages in paraxial mesoderm (pm) and in two domains lateral to the neural plate (white arrowheads). (C, D, G, H), dorsal views. Double *rhoU*/*sox9* and *rhoU*/*twist* ISH analyses show that the two *rhoU*-positive lateral domains (white arrowheads) are excluded from the presumptive NC territories that are *sox9* and *twist* positive. (I, J, K, L), dorsal views. Before migration, *rhoU* is expressed in paraxial mesoderm (pm) and otic placodes (op, white arrowheads), as revealed by double *rhoU*/*sox9* ISH analyses (K, L). (M, N), anterior views. *RhoU* is expressed in migrating CNC cells, as demonstrated by *rhoU*/*twist* ISH analyses (black arrowhead in N). (O), lateral view (P), dorsal view, (Q), lateral view. From stages 23 to 24, *rhoU* transcripts are mainly localized in migrating CNC cells (mCNC), otic vesicles (ov), pronephric ducts (pd), eyes (e) and cement gland (cg). (R), lateral view, (S), dorsal view. *RhoU* expression is maintained later on in migrating CNC cells (mCNC) and cement gland (cg). At this stage, *rhoU* expression is abundant in the tail bud (tb). (T, U), lateral views. (V), anterior view. At stage 32, *rhoU* expression is found in the pharyngeal arches (white arrow), in the cement gland (cg) and in the anterior-most hatching gland (white arrowhead in panel V).

migrate on a fibronectin substrate, through the activity of the integrin α5β1 receptor complex (Alfandari et al., 2003). This system was used previously to identify proteins whose depletion impaired CNC cell migration *in vivo* (Rangarajan et al., 2006; Nie et al., 2009; Hwang et al., 2009). As shown in Fig. 4A, control CNC explants dissected from stage 17 embryos rapidly adhered and spread on fibronectin-coated

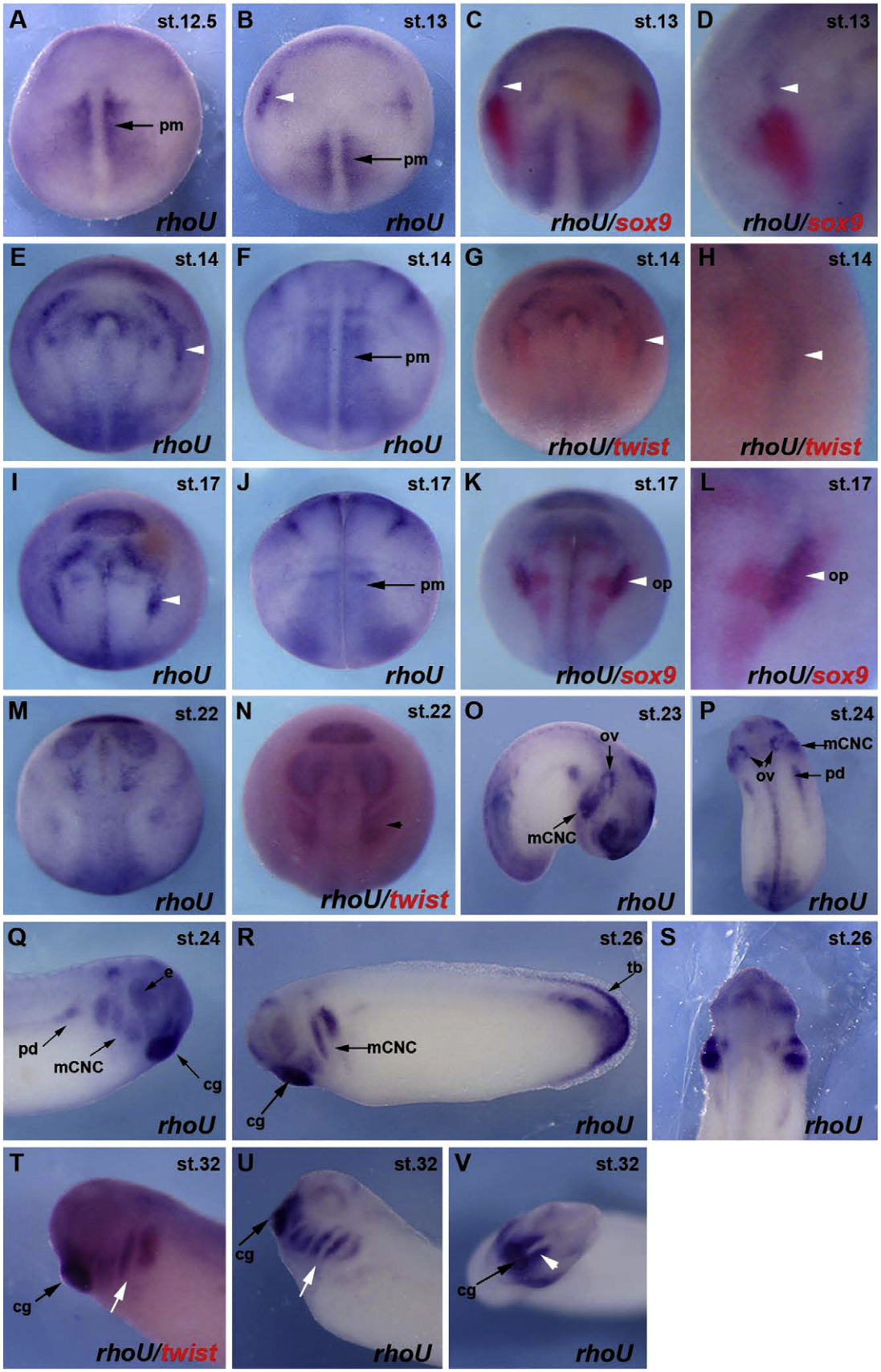

substrates. Eight hours after plating, control CNC explants segregated into several lobes, reflecting individual CNC cell streams migrating toward branchial arches *in vivo*, as previously reported (Alfandari et al., 2003). Control individual cells showed a motile morphology (Fig. 4A, upper panels) and exhibited extensive F-actin rich protrusions, such as filopodia and lamellipodia, and a leading edge to trailing edge polarity (Fig. 4B). In contrast, RhoU-MO explants failed to spread and to segment in organized lobes (Fig. 4A, middle panels). Instead,

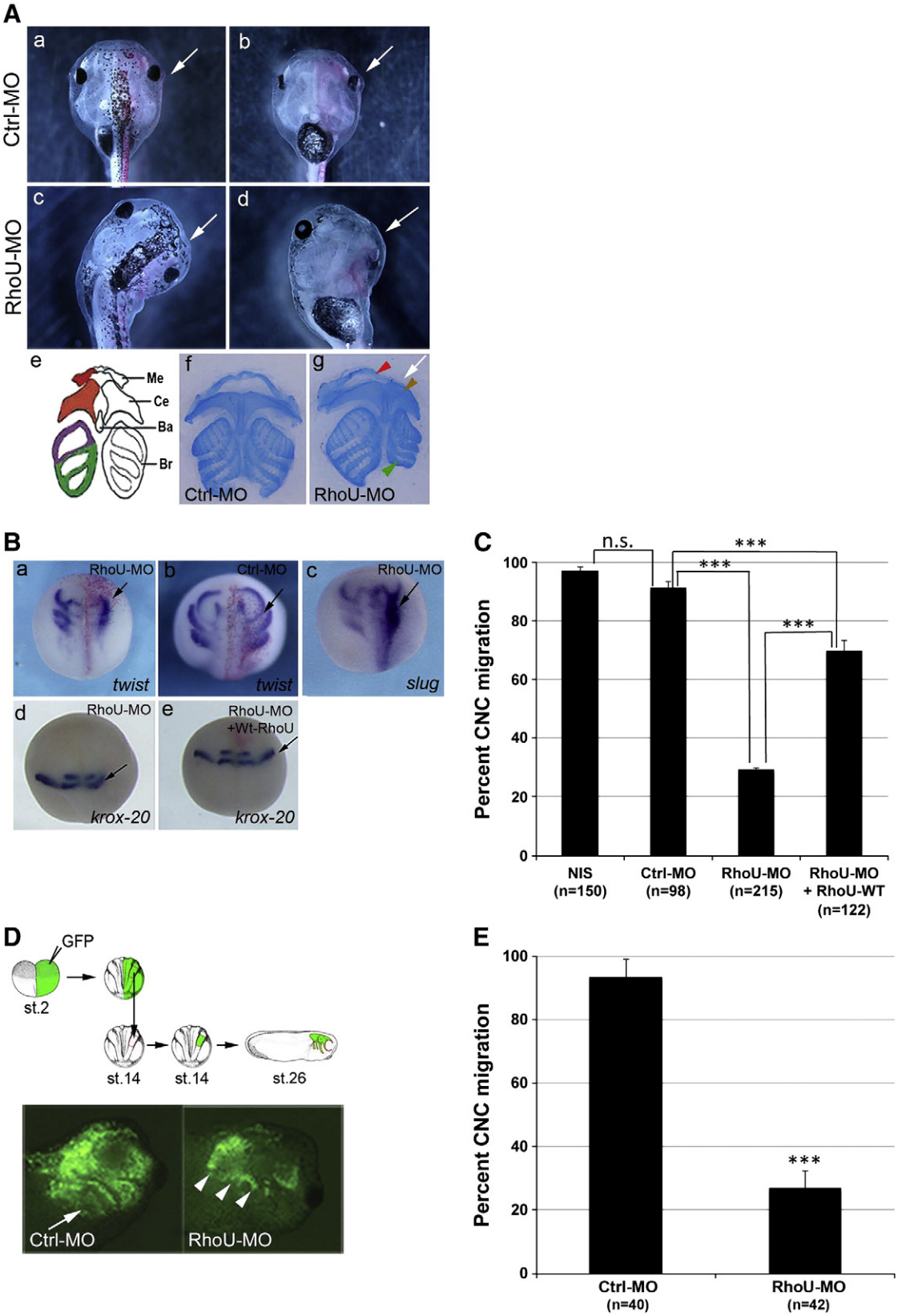

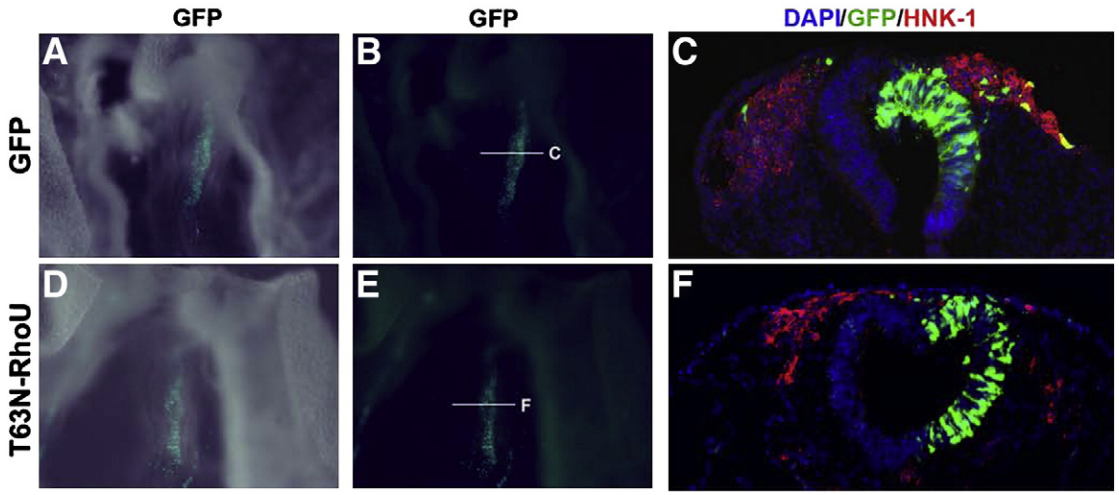

Fig. 3. RhoU loss-of-function in the chick embryo blocks CNC cell emigration and migration. Electroporations of pCAGGS-IRES-nls-GFP plasmid alone or together with pCS2-T63N-RhoU into the midbrain region of chick embryos at the 2–4 somite stage. Embryos were allowed to develop until the 9 somite stage. (A, B, D, E): whole-mount GFP stainings. (C, F): immunohistochemistry analysis of HNK-1 expression in transverse sections at levels indicated in B and E. In all panels, the electroporated side is on the right.

explants from RhoU-MO injected embryos disaggregated (100%, $n = 120$). RhoU-depleted cells poorly adhered to the fibronectin substrate and remained rounded. This was associated with a reduced number of phospho-tyrosine-positive focal complexes (Fig. 4C) and a lack of protrusions (Fig. 4B) in all examined cells ($n = 250$). These effects were significantly rescued by co-injection of a *GFP-Wt-RhoU* mRNA, with 71% of co-injected explants (57/81) exhibiting cell attachment and migration. This supports the conclusion that RhoU controls CNC cell migration *in vitro* by regulating adhesive structures required for cell attachment and spreading.

The level of RhoU activity is critical for explant polarity and directional CNC cell migration in vitro

We next investigated what could be the effect of RhoU overexpression on CNC cell migration (Fig. 5). *Xenopus* embryos were co-injected in one cell of 4–8 cell stage with *Wt-RhoU* mRNA and nβGal mRNA as a linear tracer. Embryos were then cultured until stage 22 and examined by ISH with the NC markers *slug* and *twist* and the hindbrain/NC *krox-20*. Interestingly, Wt-RhoU overexpression induced severe defects in CNC cell migration. Only 37% (87/234) of Wt-RhoU expressing embryos exhibited normal migration compared to 93% (97/105) of embryos injected with *nβGal* mRNA alone (Figs. 5A, B). Moreover, Wt-RhoU injected embryos cultured to the tadpole stage (stage 45) exhibited abnormal head morphology (data not shown). Like for RhoU depletion, the migration defects induced by Wt-RhoU overexpression were cell autonomous (Figs. 5 C, D). Analysis of embryos at early specification stages showed that Wt-RhoU expression, like that of Wt-RhoV, induced a marked expansion of the territory positive for *snai1/snail* (62%, $n = 46$), *sox9* (71%, $n = 61$) and *snai2/slug* (68%, $n = 43$) (Supplemental Fig. 2). This effect probably results from activation of RhoV targets, since RhoU, normally not expressed at early specification stages, can complement RhoV depletion (Guemar et al., 2007). However, since RhoV overexpression had no effect on CNC cell migration, the inhibition of migration elicited by Wt-RhoU is probably independent of its effect on specification.

To address whether the mechanisms by which loss-or gain-of RhoU function affect CNC cell migration are similar, we examined the behavior of CNC explants from Wt-RhoU expressing *Xenopus* embryos *in vitro*. As shown in Fig. 6A, eight hours after plating, CNC cells from Wt-RhoU-injected explants adhered to the substrate and scattered more rapidly than control explants. Cell scattering also appeared isotropic whereas it was clearly oriented in control explants, which suggests that RhoU activity impacts on polarity. We thus tracked by video-microscopy individual CNC cells detaching from the explants and compared their migration paths (see Fig. 6B and Supplemental movies). Cell tracking showed no significant differences in the total traveled distances between control and Wt-RhoU expressing cells (Fig. 6 C). However, linear motions of cells (Fig. 6D) and directionality of their migration (expressed as persistence, i.e. the ratio of the linear distance to the total distance traveled by a cell) (Fig. 6E) were significantly reduced in Wt-RhoU expressing cells. Last, Wt-RhoU-injected cells, either individual or located at the explant border, displayed extensive protrusions – mainly large lamellipodia – all

Fig. 2. *rhoU* mRNA is expressed in *Xenopus* migrating CNC cells and is required for migration. (A) RhoU knock-down elicits the loss of neural crest derivatives. 4–8 cell stage *Xenopus* embryos were injected with nuclear β-galactosidase mRNA plus control MO (Ctrl-MO) or RhoU-MO and then fixed at stage 45. Shown are Ctrl-MO (a, b) and RhoU-MO-injected embryos (c, d) representative of the observed skeletal defects. Dorsal views (a, c), ventral views (b, d). The injected side is on the right, as monitored by the co-injected β-galactosidase mRNA lineage tracer (red staining) and indicated by white arrows. (e) Drawing of ventral cranial cartilages modified from Sadaghiani and Thiebaud (1987) and Spokony et al. (2002). Neural crest derived cartilages are marked as: Me, Meckel's cartilage; Ce, cerathoyal cartilage; Ba, basihyal cartilage; Br, branchial/gill cartilage. (f, g) Skeletal structures from Ctrl-MO (f) and RhoU-depleted (g) stage 45 tadpoles were stained with alcian blue on flat-mount embryos. Arrows in g use the same color code as in e. (B) RhoU knock-down impairs CNC cell migration. 4–8-cell stage embryos were co-injected into a single cell with nuclear β-galactosidase mRNA plus control MO (Ctrl-MO) or RhoU-MO. Dorsal views of stage 22 embryos, injected sides (red staining) are on the right. (a) *Twist* and (c) *slug* and stainings on RhoU-MO injected embryos. (b) *Twist* staining on control MO (Ctrl-MO) injected embryo. RhoU depletion inhibits CNC cell migration into pharyngeal arches (black arrows). (c) *Krox-20* ISH showed that CNC cells did not migrate into the third branchial arch in RhoU-MO morphants, while expression in the hindbrain was not affected. (d) Co-injection of 200 pg *GFP-Wt-RhoU* mRNA, insensitive to RhoU-MO, rescued CNC cell migration, as evidenced by the *krox-20* staining in the third branchial arch (black arrow). (C) Graph summarizing the results of three independent injection experiments as described in B. NIS, non-injected control side; Ctrl-MO, control side injected with control MO; n, total number of embryos analyzed. *** indicates conditions statistically different ($p < 0.001$). (D) RhoU function in the CNC cell is cell-autonomous. 4–8-cell stage embryos *Xenopus* embryos were injected in one cell with 300 pg *GFP* mRNA plus control MO (Ctrl-MO) or RhoU-MO. At early neurula stages, correctly targeted embryos were identified using a fluorescence-equipped dissecting microscope. CNC explants were then grafted into uninjected control embryos, as schematized. CNC cell migration was normal in GFP grafts (white arrow) while it was impaired in RhoU-depleted grafts (white arrowheads). (E) Graph summarizing the results of three independent graft experiments as described in D. NIS, non-injected-side; n, total number of embryos analyzed. *** indicates conditions statistically different ($p < 0.001$).

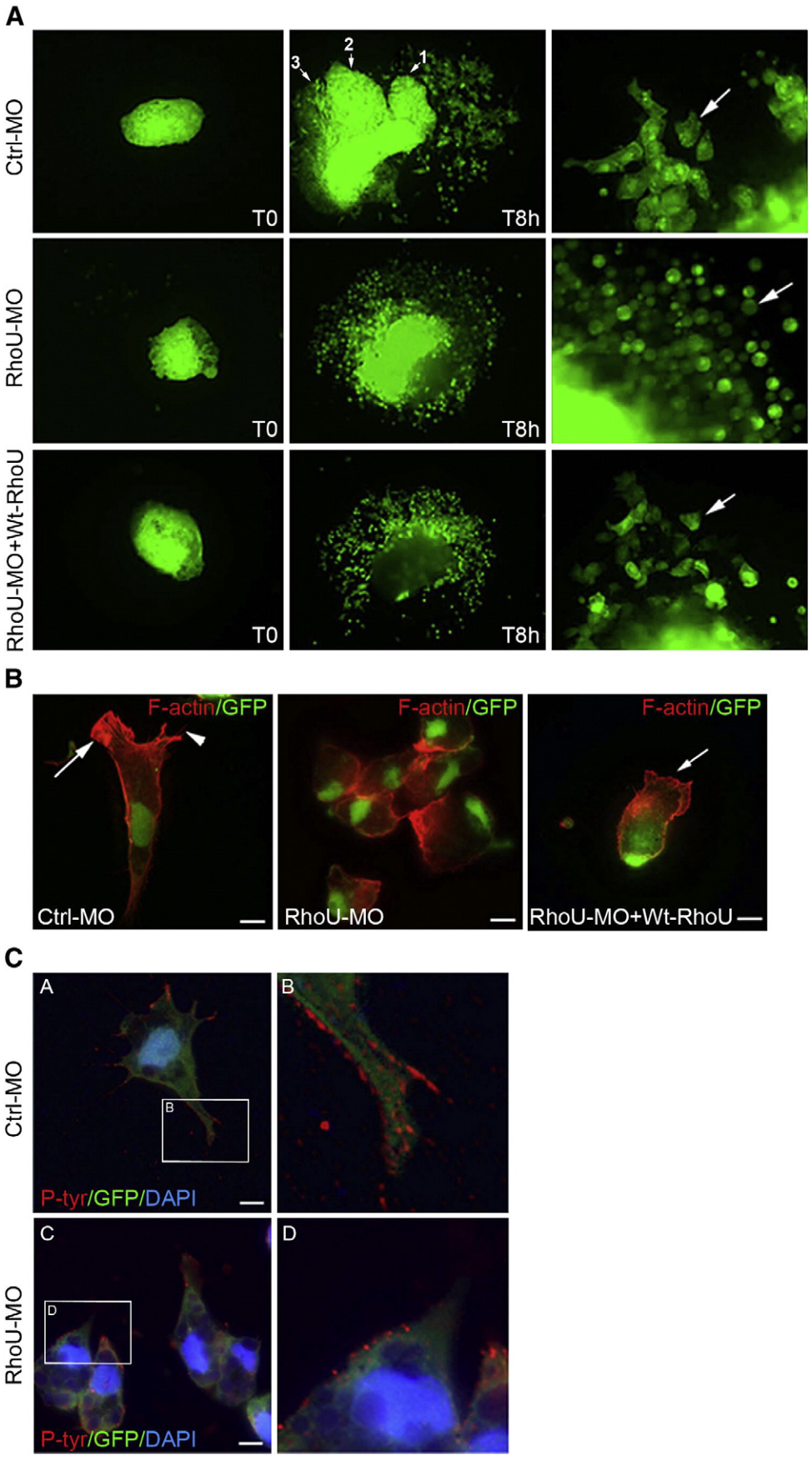
A
Ctrl-MO
RhoU-MO
RhoU-MO+Wt-RhoU
T0
T8h
1
2
3
B
F-actin/GFP
Ctrl-MO
RhoU-MO
RhoU-MO+Wt-RhoU
C
A
B
C
D
P-tyr/GFP/DAPI

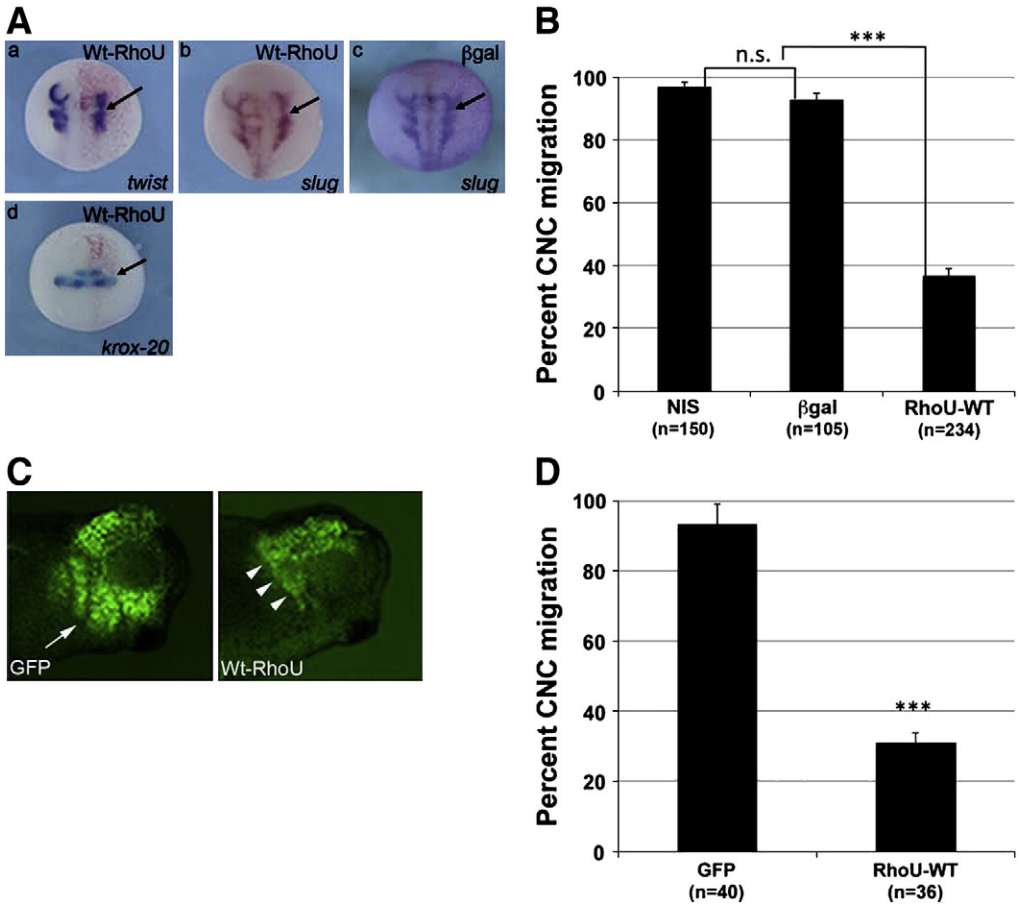

Fig. 5. Wt-RhoU overexpression impairs CNC cell migration. (A) Embryos were injected with nuclear β-galactosidase mRNA (βgal) alone or co-injected with 225 pg *Wt-RhoU* mRNA and analysed at stage 22. Dorsal views of stage 22 embryos, injected sides (red staining) are on the right. (a) *twist*, (b) *slug* and (d) *krox-20* stainings on embryos injected with Wt-RhoU. (c) Control *slug* staining on embryos injected with nuclear β-galactosidase (βgal) mRNA alone. RhoU overexpression induced severe CNC cell migration defects (black arrows). Note that *krox-20* expression in the hindbrain was unaffected. (B) Shown is a graph summarizing the results of four independent experiments as described in (A). NIS, non-injected side; β-gal, control side injected with nuclear β-galactosidase mRNA; n, total number of embryos analyzed. *** indicates conditions statistically different ($p<0.001$). (C) Embryos were injected with 300 pg *GFP* mRNA alone or with 225 pg *Wt-RhoU* and CNC explants were excised as in Fig. 2D. Cells from control GFP grafts exhibited normal migration (white arrow), whereas cells grafts from Wt-RhoU-injected embryos did not migrate properly (white arrowheads). (D) Shown is a graph summarizing the results of four independent experiments as described in (C). GFP, control side injected with *GFP* mRNA; n, total number of embryos analyzed. *** indicates conditions statistically different ($p<0.001$).

around their periphery, while cells from control explants exhibited filopodia and smaller lamellipodia at few locations only (Fig. 6 F).

RhoU controls CNC cell migration through PAK- and Rac-dependent pathways

P21 activated kinases (PAKs) participate in cell adhesion and motility and are known effectors for several Rho members including RhoU (Saras et al., 2004). To address their roles in RhoU-dependent CNC cell migration, we examined which PAK members are expressed in CNC by ISH and found that the group 1 *X-pak1* and to a lesser extent *X-pak2* mRNAs were expressed in migrating CNC cells (Supplemental Fig. 3A). Treatment of CNC explants with IPA-3, a group 1 PAK inhibitor (Deacon et al., 2008), impaired *in vitro* cell migration and formation of protrusions (Supplemental Fig. 3B). This was further supported by expression of a mutant of X-PAK1 (KR-PAK1), which acts as a dominant-negative kinase and blocks endogenous X-PAK1 activation (Wu et al., 2007). Expression of KR-PAK1 inhibited CNC cell migration. Only 34% (23/68) of KR-PAK1 injected embryos exhibited normal *krox-20* expression in the third branchial arch compared to 93% (97/105) of embryos injected with *nβGal* mRNA alone (Figs. 7A, B). It also inhibited protrusions and migration in cells from explants (Fig. 7 C), thus mimicking the RhoU-MO phenotype. Conversely, expression of a constitutively active X-PAK1 mutant (DE-PAK1) elicited a phenotype similar to the one observed upon Wt-RhoU over-expression: it induced CNC cell migration defects. 30% (17/56) of DE-PAK1 injected embryos exhibiting normal migration (Figs. 7A, B), whereas in explants, cells rapidly adhered to the substrate, spread and developed large lamellipodia at the periphery (Fig. 7C). RhoU and X-PAK1 functional interaction were supported by rescue experiments. When Wt-RhoU and KR-PAK1 were coexpressed, CNC cell migration was rescued, with 63% (65/104) of embryos exhibiting normal

Fig. 4. RhoU is required for CNC cell explants to spread and segregate on fibronectin matrix. (A) *Xenopus* embryos were injected in one cell of two-cell stage with 300 pg *GFP* mRNA plus control MO (Ctrl-MO) or RhoU-MO. At stage 17, CNC explants were excised as described (Alfandari et al., 2003) and plated on fibronectin-coated substrates. Shown are images at plating (T 0) and 8 h later (T 8 h). By 8 h, control-MO expressing explants (upper panels) spread extensively and segregated into three lobes. However, RhoU-MO-injected explants failed to spread on fibronectin substrate but dissociated into loose and rounded cells (middle panels). Co-injection of 225 pg *GFP-Wt-RhoU* mRNA partially rescued the effect (lower panels). (B) Analysis of CNC cell protrusions. Staining for GFP (green) and F-actin (red) were merged. Arrows indicate lamellipodia and arrowheads filopodia. All RhoU-MO-injected cells analyzed showed the same phenotype. Co-injection of *GFP-Wt-RhoU* mRNA restored protrusions in RhoU-MO depleted embryos. Bar, 10 μM. Co-injected cells shown are representative of 68% observed cells ($n=150$). (C) Analysis of CNC focal adhesions in control MO (Ctrl-MO) (panel A) and RhoU-MO (panel C) embryos. Staining for phosphotyrosine (red), GFP (green), and DAPI (blue) were merged. Panels B and D show higher magnifications of the boxed areas of panels A and C, respectively. RhoU-MO-injected cells shown are representative of 82% observed cells ($n=150$). Bar, 10 μM.

migration compared to 37% and 34% with Wt-RhoU and KR-PAK1 alone, respectively (Figs. 7A, B). This suggests that failure of CNC cell migration in Wt-RhoU expressing embryos is relieved by reducing the level of PAK1 activity. Since PAK activity is also associated with that of Rac1, the major regulator of lamellipodia (Jaffe and Hall, 2005), we investigated the functional relationship between RhoU and Rac1 in

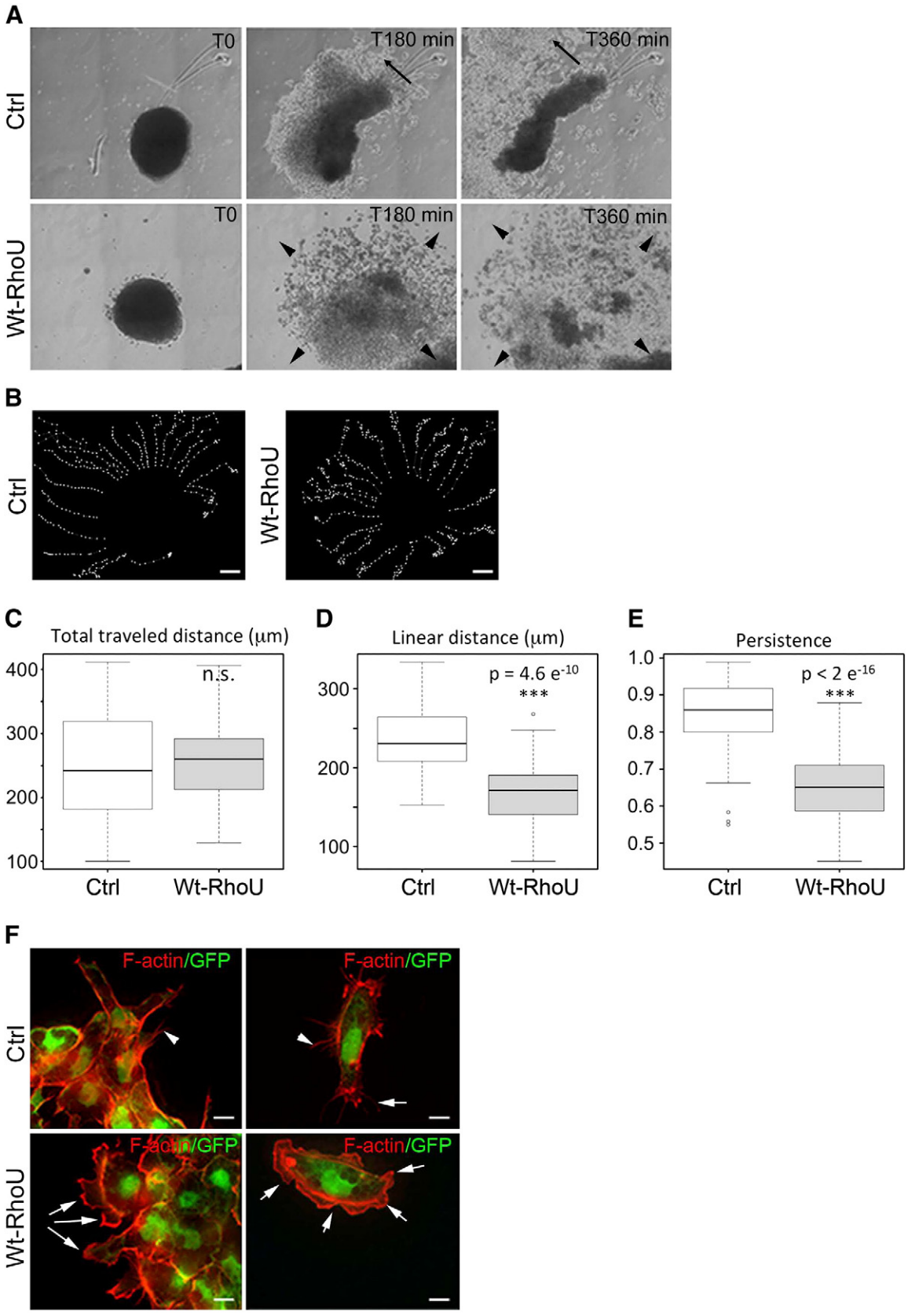

CNC cell migration. Like RhoU depletion or IPA-3 treatment, treatment of CNC explants with the Rac inhibitor NSC23766 (Gao et al., 2004) inhibited cell migration and formation of protrusions (data not shown). Like Wt-RhoU, expression of Wt-Rac1 also inhibited CNC cell migration (27% of embryos exhibiting normal CNC cell migration). Given the similarities between RhoU and Rac1 phenotypes, we examined the ability of Rac1 to rescue the loss of RhoU activity. As shown in Figs. 7A and B, Wt-Rac1 over-expression rescued CNC cell migration in RhoU-MO injected embryos, as monitored by 57% (91/160) of embryos showing *krox-20* positive CNC cells on the injected side and by the reappearance of protrusions in cells migrating from explants (Fig. 7D). Our data therefore suggest that PAK- and Rac-dependent pathways contribute to the formation of protrusions and subsequent migration of CNC cell downstream of RhoU.

Discussion

In the recent years, the neural crest has attracted much attention for its stem cell-like properties (Nagoshi et al., 2009) and its capacity to switch from an epithelial state to a highly invasive mesenchymal phenotype (Thiery et al., 2009). Considerable progress has been made toward the understanding of the molecular mechanisms that control NC cell physiology, in particular the importance of Wnt, BMP and FGF signalings in specification (Sauka-Spengler and Bronner-Fraser, 2008). Given their pivotal roles on basic cell properties such as adhesion, migration and polarity, Rho-controlled pathways have been studied in NC development and shown to participate in self-renewal (Rac and Cdc42, Fuchs et al., 2009), specification (Rac1, Broders-Bondon et al., 2007; RhoV, Guemar et al., 2007), delamination (RhoA–C, Groysman et al., 2008; RhoB, Liu and Jessell, 1998) and migration (Trio, Kashef et al., 2009; Rac1, Matthews et al., 2008; RhoA, Rupp and Kulesa, 2007). These studies have mainly focused on RhoA, Rac and Cdc42, the most conserved and expressed members, whereas the Rho family in vertebrates is more complex, since it contains 15 to 18 additional members of poorly known functions (Boureux et al., 2007). This is the first *in vivo* study of the functional role of RhoU in a vertebrate embryo. We show here that the non-canonical Wnt response *rhoU* gene is early expressed in *Xenopus* CNC cells migrating towards the forming branchial arches. Using gain- and loss-of-function analysis, we provide the first evidence that RhoU is an essential regulator of CNC cell migration *in vivo*. The level of RhoU expression appears critical since depletion and overexpression both induce severe migration defects and subsequent abnormal differentiation of CNC cell into cranial cartilages.

RhoU and RhoV are two closely related members that delineate a Rac/Cdc42 subclass emerged in early multicellular animals (Boureux et al., 2007). These two GTPases enhance PAK and JNK activities, localize to focal adhesions and exhibit transforming activity (Aronheim et al., 1998; Berzat et al., 2005; Chuang et al., 2007; Tao et al., 2001; Weisz Hubsman et al., 2007). In contrast with classical Rho, Rac and Cdc42 members, RhoU and RhoV exchange GTP spontaneously (Saras et al., 2004; Shutes et al., 2006) and their activity is thus directly associated with their levels of expression. In *Xenopus*, RhoV is transiently induced shortly after gastrulation in the prospective neural crest-forming region and is required for the induction of *snai2/slug*, *twist* or *sox9* mRNAs downstream of Snai1/Snail (Guemar et al., 2007). RhoU is induced in NC cells after RhoV extinction and is required for adhesion and migration. Despite these similarities, the two GTPases are not structurally and functionally equivalent: RhoU contains in its N-terminus an SH3-binding domain not detected in RhoV amino-acid sequence, and although RhoU has the capacity to complement RhoV knockdown in CNC specification (Guemar et al., 2007), RhoV did not rescue migration defects in RhoU morphant embryos (data not shown). This situation is reminiscent of the closely related Sox8 and Sox10 transcription factors, which can substitute each other in many developmental processes except for melanocyte differentiation (Kellerer et al., 2006). Another major difference between RhoU and RhoV lies in their activating pathways, since *rhoV* gene expression is spatially and temporally restricted and activated by the β-catenin dependent canonical Wnt pathway (Boureux et al., 2007; Guemar et al., 2007) whereas *rhoU* expression is more ubiquitous and controlled by the non-canonical Wnt pathway and Stat3-dependent inflammatory signals (Schiavone et al., 2009; Tao et al., 2001).

RhoU was previously shown to stimulate the formation of filopodia in endothelial and fibroblastic cells (Aspenstrom et al., 2004; Tao et al., 2001). In CNC cells, RhoU overexpression clearly induced the formation of lamellipodial structures. Similar situations were reported for Cdc42, capable of activating formation of either structure depending on the cell type used for the assay (reviewed in Jaffe and Hall, 2005). Furthermore, the capacity of Cdc42 and other GTPases such as TCL and RhoG to induce lamellipodia was shown to require Rac activity (Gauthier-Rouviere et al., 1998; Vignal et al., 2000). This is also the case for RhoU, since treatment with the Rac inhibitor NSC23766 blocked the formation of lamellipodia in RhoU overexpressing CNC cells (data not shown).

Our *in vitro* results strongly suggest that the migration defects observed upon RhoU knockdown are underlaid by a dramatic loss of cell–cell and focal adhesion whereas those observed upon RhoU overexpression mainly affect polarity of migration. This suggests that low levels of RhoU expression are required for cell–cell and focal adhesion, while higher levels might influence polarity of cell migration. Our data thus support previous reports which implicate RhoU activity in the formation and distribution of focal adhesions in fibroblasts and adherens and tight junctions in epithelial cells (Brady et al., 2009; Chuang et al., 2007; Ory et al., 2007), as well as in the migration of cultured osteoclasts (Brazier et al., 2009). Most of these data also pointed to phenotypic similarities between depletion and overexpression, supporting further our findings that RhoU exerts its optimal physiological activity within a narrow expression range.

How RhoU control both cell–cell junctions and focal adhesion remains to be clarified. RhoU might interact with distinct effectors, eliciting different cell outcomes. RhoU was shown to interact with group I PAKs, ubiquitous S/T kinases activated by all Rac/Cdc42-like members (Saras et al., 2004), and Pyk2, a non-receptor tyrosine kinase mostly expressed in epithelial cells, neurons and cells of the hemopoietic lineage (Ruusala and Aspenstrom, 2008). These two kinase types are known regulators of epithelial cell spreading and motility. PAK members localize to focal adhesions via the PIX/GIT/Paxillin complex (Brown et al., 2002; Manabe et al., 2002; Zhao et al., 2000) and activate cell spreading and migration (Symons, 2000). PAK1 and PAK2 were recently shown to control two distinct focal adhesion pathways, both necessary for breast carcinoma cell invasion (Coniglio et al., 2008). PAK1 represents an interesting candidate, since its mRNA accumulates in migrating CNC cells

Fig. 6. RhoU regulates the directionality of CNC cell migration *in vitro*. Embryos were injected with 300 pg *GFP* mRNA alone (control, Ctrl) or with 225 pg *Wt-RhoU* mRNA. At stage 17, CNC explants were excised and plated on fibronectin-coated substrates. (A) Time-lapse microscopy images of explants at plating (T 0) and 3 (T 180 min) and 6 h (T 360 min) thereafter. Arrows in the top panels indicate the preferential direction of migration of control CNC cells, while arrowheads in the bottom panels illustrate the multiple directions followed by RhoU-expressing cells. (B) Behavior of labeled cells in CNC explants was recorded by time-lapse movies. Paths followed by control and Wt-RhoU expressing cells during a 6-hour migration. Bar, 20 μM. (C, D, E) Trajectories of individual cells from two control (Ctrl) explants ($n_1 = 21$ and $n_2 = 22$) and three Wt-RhoU expressing explants ($n_1 = 21$, $n_2 = 23$ and $n_3 = 23$) were tracked. Total distance traveled (C), linear distance traveled (D) and persistence index (E) were calculated. Graphs show box-and-whiskers plots for all conditions. *** indicates statistically significant differences. n.s.: not significant. (F) Analysis of CNC cell protrusions. Staining for GFP (green) and F-actin (red) were merged. Left panels show cells located at the explant border while right panels show individual motile cells. Arrows point to lamellipodia and arrowheads indicate filopodia. Wt-RhoU expressing cells shown are representative of 72% observed cells ($n = 160$). Bar, 10 μM.

(Supplemental Fig. 3). On the other hand, Pyk2 knockdown was shown to induce spreading and motility of prostate epithelial cells (de Amicis et al., 2006), associated with E-cadherin inhibition and alpha5 integrin induction. Pyk2 is also a critical mediator of anchorage-independent growth and anoikis resistance of immortalized corneal epithelial cells (Block et al., 2010). Interaction with Pyk2 may also mediate the functional specificities of RhoU vs. RhoV, since it requires the presence of the SH3-binding domain (Ruusala and Aspenstrom, 2008). Given their impact on cell spreading and motility, PAK and Pyk2 thus represent interesting candidates as RhoU effectors that might control the balance between cell-cell junctions and focal adhesion. However, other targets such as Myosin-X, critical for CNC cell migration in *Xenopus* (Hwang et al., 2009; Nie et al., 2009) might also participate in the balance, since RhoU was shown previously to control formation of focal adhesions through myosin phosphorylation (Chuang et al., 2007).

Recent modeling of the impact of Wnt signaling on migration of mesoderm explants showed that explant polarity and direction of migration depend on two main parameters, i.e. cell polarity and cadherin–integrin balance (Robertson et al., 2007). This fits well the hypothesis that RhoU impacts on the balance between cell–cell and cell–extracellular matrix adhesion, which would then affect explant polarity and cell directionality. Alternately, since directional cell migration also depends on the orientation of cell protrusions (Ridley et al., 2003), the reduced directionality observed in Wt-RhoU expressing cells may be a direct consequence of an excess of unpolarized lamellipodia. This supports the observation that

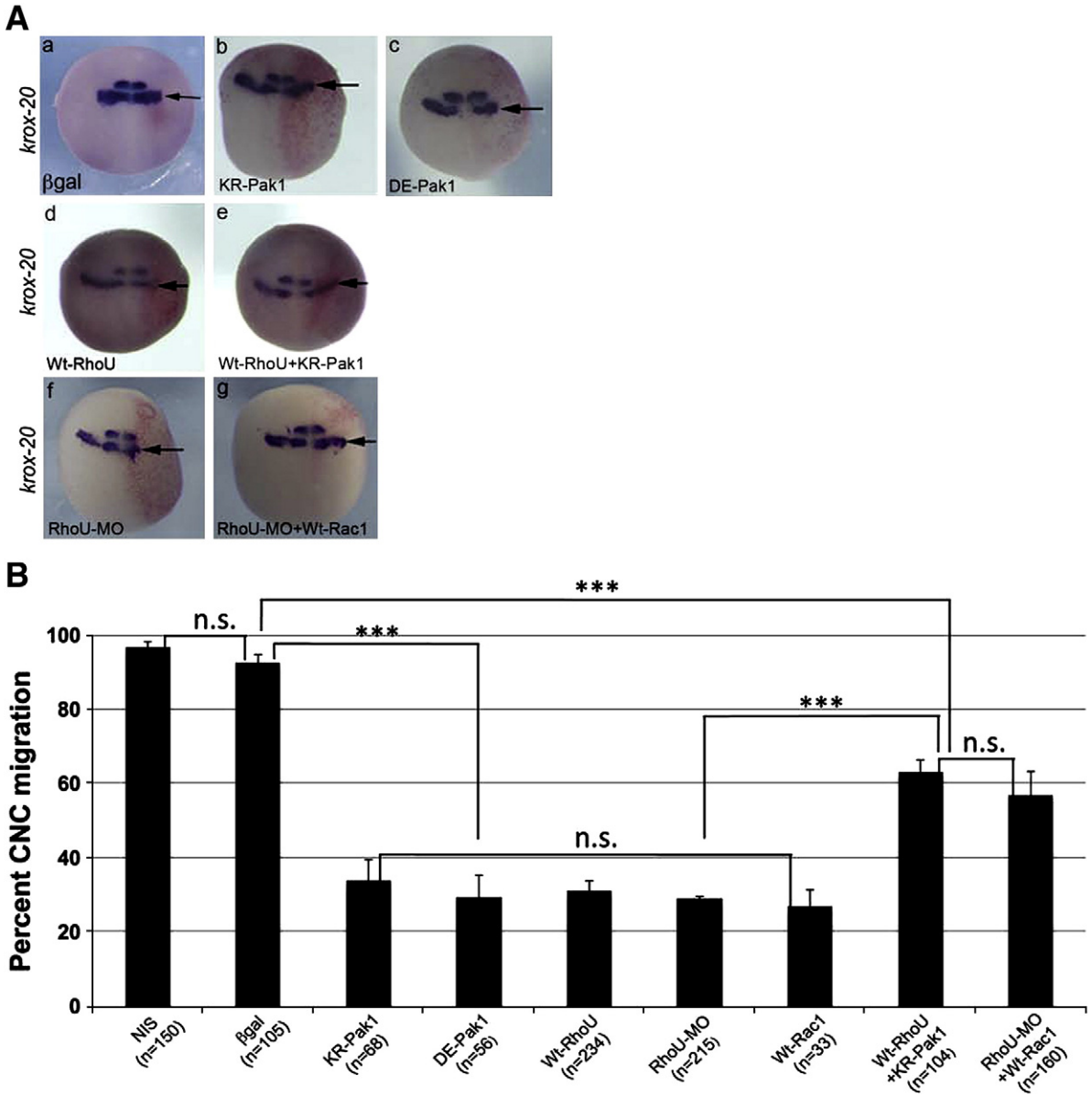

Fig. 7. RhoU controls CNC cell migration through PAK- and Rac-dependent pathways. (A) *krox-20* whole-mount ISH analysis. Embryos were injected, fixed at stage 22 and processed for ISH. Embryos were injected with (a) 200 pg nuclear β-galactosidase mRNA (βgal), (b) 400 pg *KR-Pak1* mRNA, (c) 200 pg *DE-Pak1* mRNA, (d) 225 pg *Wt-RhoU*, (e) 225 pg *Wt-RhoU* with 400 pg *KR-Pak1* mRNAs, (f) 20 ng RhoU-MO, *(g)* 20 ng RhoU-MO with 80 pg *Wt-Rac1* mRNA. Nuclear β-galactosidase was used as a lineage tracer. Dorsal views, injected sides (red staining) are on the right. (B) Graph summarizing the results of four independent experiments as described in (A). NIS, non-injected-side; n, total number of embryos analyzed. ***($p<0.001$) indicates statistically different conditions. n.s.: not significant. (C) Analysis of CNC cell protrusions. CNC explants from embryos injected as in (A) were excised at stage 17 and plated on fibronectin-coated substrates. Staining for GFP (green) and F-actin (red) were merged. Arrows indicate lamellipodia and arrowheads filopodia. KR-PAK1 expressing cell shown is representative of 85% observed cells ($n=160$). DE-PAK1 expressing cell shown is representative of 69% observed cells ($n=140$). Bar, 10 μM. (D) Cells from RhoU-MO or RhoU-MO+ Wt-Rac1 mRNA-injected embryos. GFP (green) and F-actin (red) staining were merged. Arrows indicate lamellipodia. Co-injected cells shown are representative of 56% observed cells ($n=140$). Bar, 10 μM.

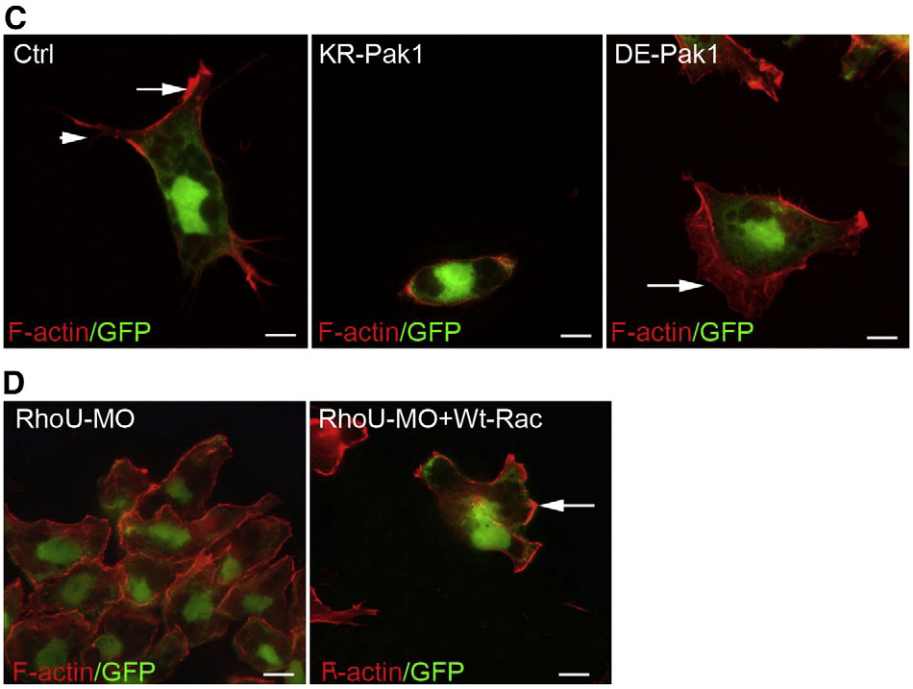

Fig. 7 (*continued*).

lamellipodia formed in RhoU overexpressing cells are Rac1 and PAK-dependent, know to be critical for cell polarity (Petrie et al., 2009).

In conclusion, our findings raise new issues on how two related atypical Rho GTPases couple cell differentiation, adhesion and migration in normal physiological processes. In addition to RhoV, previously shown to interplay with Snai1/Snail in Wnt-stimulated CNC cell specification, we show here that RhoU controls subsequent CNC polarity, adhesion and migration. Since Wnt signalings are frequently over-activated in many cancer types, this opens new perspectives on the pro-invasive roles of these two GTPases in malignant transformation, in particular during the early steps of tumor progression.

Materials and methods

Isolation of Xenopus RhoU

Xenopus laevis RhoU cDNA sequences (BC077840 or BC078037) were identified by blast searches. Alignment of *Xenopus laevis*, human and rat RhoU and RhoV (the closest RhoU relative) protein sequences was previously reported (Guemar et al., 2007). RhoU ORF was obtained by RT-PCR amplification of stage 23 embryo mRNA using specific primers (forward 5′-CCG AAT TCG GCA GAT ACA AAA TGC CAC CTC AAG TGA TG-3′; reverse 5′-CCC TCG AGC CCT TGT GGT CGT CAT TC-3′), cloned into the EcoR1/Xho1 sites of the pCS2+ vector and checked on an ABI310 automatic sequencer (Perkin-Elmer, Foster City, USA).

DNA constructs and mRNAs synthesis

Xenopus Rac1 ORF was amplified by RT-PCR and cloned in pCS2+. pCS2-KR-PAK1 and pCS2-DE-PAK1 were previously described (Wu et al., 2007). Synthetic-capped mRNAs were generated using the mMessage mMachine kit (Ambion). Human Wt and T63N-RhoU were cloned in pCS2+ from the original pRK5 constructs (Saras et al., 2004).

Xenopus and chick embryos manipulation and morpholino oligonucleotides

Xenopus laevis embryos were obtained by *in vitro* fertilization, grown as previously described (Faure et al., 2000) and staged according to Nieuwkoop and Faber (Nieuwkoop and Faber, 1967). Morpholino antisense oligonucleotides (MO) were obtained from Gene Tools (Philomat, USA). RhoU-MO, designed to target the translation–initiation site of RhoU (position +2 to +26 relative to the translational star of *Xenopus* RhoU) were previously characterized (Guemar et al., 2007). A randomized antisense oligonucleotide (Ctrl-MO) was used as a control sequence. MOs were injected into dorsal animal region of 4–8 cell stages embryos at the same concentration (20 ng per embryo). Nuclear β-galactosidase mRNA was injected at 200 pg per embryo.

Xenopus cranial neural crest (CNC) explants were dissected from stage 14 to 17 embryos and either transplanted or plated onto fibronectin (FN, 30 mg/ml in PBS-coated dishes in DFA media, Alfandari et al., 2003). The group I PAK inhibitor IPA-3 (Sigma) was used at 7 μM in DMSO (0.025% final dilution). The Rac inhibitor NSC23766 (Tocris Biosciences, UK), shown to have no effect on RhoA or Cdc42 activation, was used at 10 μM.

Fertilized White Leghorn eggs were obtained from Haas Farm (France), incubated at 38 °C in a humidified incubator and embryos were staged (HH, reprinted in Hamburger and Hamilton, 1992). The pCAGGS-IRES-nls-GFP plasmid was injected alone or co-injected with the pCS2-T63N-RhoU into the lumen of chick embryos at the 2–4 somite stage (ss), at the level of the midbrain region, and electroporated using standard protocols (Cheung et al., 2005). Embryos were collected 8 h later and immunostained for HNK-1 to monitor possible changes in neural crest cell migration as previously reported (Coles et al., 2007).

In situ hybridization, immunochemistry, imaging

Single and double *in situ* hybridization (ISH) analyses were performed as described (Vignal et al., 2007). Cartilages were stained

as previously reported (Guemar et al., 2007). For immunostaining, CNC explants were fixed in 4% PFA for 10 min, permeabilized in 0.1% Triton X-100 in PBS and stained with phalloidin-TRITC for F-actin or with anti-phospho-tyrosine (Tebu-Bio) and Alexa555 anti-mouse (Invitrogen) antibodies. Avian embryo sections were processed with anti-HNK-1 (CD57 Ab2, NeoMarker) and Alexa 488 anti-mouse (Invitrogen) antibodies and mounted in FluorSave reagent (Calbiochem). GFP signal was observed under direct excitation. Sections were visualized by fluorescence microscopy (AX10 Imager.M1, Zeiss) and images captured with an AxioCam MRm camera (Zeiss).

Statistical analysis of embryo phenotypes

For each condition (i.e. injected mRNA or morpholino), three to five independent experiments were performed and embryos with normal or defective neural crest migration were counted. We used Fisher's exact tests to check homogeneity of variance within each condition and a generalized linear model (GLM) with a binomial link function for pairwise comparisons between conditions (***$p<0.001$, NS $p>0.05$). Calculations were performed using the R free software (R Development Core Team, 2004).

Live imaging and cell tracking

CNC explants were plated on fibronectin coated dishes and live cell imaging was performed at 25 °C using a Leica DMIRE2 inverted microscope coupled to a Micromax HS1300 camera (Roper Scientific). Images were acquired in stitching mode (3×3) every 15 min (for a total duration of 390 min) with a 20× phase air objective (exposure time 30 ms). To evaluate the persistence index, images stacks were processed with Metamorph (Universal Imaging). For each explant (two control and three RhoU expressing ones) 21 to 23 individual cells were tracked. Movies were finally edited with ImageJ.

For each explant, normal distributions of cell paths and persistence data were analyzed using a GLM with a Gaussian link function: Persistence = Condition, where Persistence is a continuous response variable (the ratio between the linear distance and total distance traveled by each cell of each explant) and Condition a categorical explanatory variable with five levels corresponding to each explant. Normality of the GLM residuals was validated by a Shapiro–Wilk test ($/W/=0.98$ and $/p/=0.09$). Step-wise analysis was performed using /*F*/-tests to test for differences in persistence between conditions, by grouping levels starting from the less different ones. No significant variations were detected between the two control explants or between the three Wt-RhoU expressing explants (/*F*/-values ranging from 0.1 to 1.1; /*p*/ 0.3–0.7). However, persistence values were significantly higher in controls than in Wt-RhoU expressing explants (/*F*/-value = 86.89; $/p/<2.e^{-16}$ ***). Statistical analyses and box-and-whiskers plots were computed using the R free software (R Development Core Team, 2004).

Supplementary materials related to this article can be found online at

Acknowledgments

The authors would like to thank Cell Signalling Department members for valuable discussions, in particular Anne Blangy for critical reading of the manuscript. We also thank Olivier Duron and Pierrick Labbé (ISEM, UMR5554) for help in statistical analysis with the R software. This work was supported by CNRS institutional grants and contracts from the Association pour la Recherche contre le Cancer (ARC no. 3753 and no. 1048) and from the Ligue Régionale contre le Cancer.

References

Alfandari, D., Cousin, H., Gaultier, A., Hoffstrom, B.G., DeSimone, D.W., 2003. Integrin alpha5beta1 supports the migration of Xenopus cranial neural crest on fibronectin. Dev. Biol. 260, 449–464.
Aronheim, A., Broder, Y.C., Cohen, A., Fritsch, A., Belisle, B., Abo, A., 1998. Chp, a homologue of the GTPase Cdc42Hs, activates the JNK pathway and is implicated in reorganizing the actin cytoskeleton. Curr. Biol. 8, 1125–1128.
Aspenstrom, P., Fransson, A., Saras, J., 2004. Rho GTPases have diverse effects on the organization of the actin filament system. Biochem. J. 377, 327–337.
Berzat, A.C., Buss, J.E., Chenette, E.J., Weinbaum, C.A., Shutes, A., Der, C.J., Minden, A., Cox, A.D., 2005. Transforming activity of the Rho family GTPase, Wrch-1, a Wnt-regulated Cdc42 homolog, is dependent on a novel carboxyl-terminal palmitoylation motif. J. Biol. Chem. 280, 33055–33065.
Block, E.R., Tolino, M.A., Klarlund, J.K., 2010. Pyk2 activation triggers epidermal growth factor receptor signaling and cell motility after wounding sheets of epithelial cells. J. Biol. Chem. 285, 13372–13379.
Boureux, A., Vignal, E., Faure, S., Fort, P., 2007. Evolution of the Rho family of ras-like GTPases in eukaryotes. Mol. Biol. Evol. 24, 203–216.
Bradley, L.C., Snape, A., Bhatt, S., Wilkinson, D.G., 1993. The structure and expression of the Xenopus Krox-20 gene: conserved and divergent patterns of expression in rhombomeres and neural crest. Mech. Dev. 40, 73–84.
Brady, D.C., Alan, J.K., Madigan, J.P., Fanning, A.S., Cox, A.D., 2009. The transforming Rho family GTPase Wrch-1 disrupts epithelial cell tight junctions and epithelial morphogenesis. Mol. Cell. Biol. 29, 1035–1049.
Brazier, H., Pawlak, G., Vives, V., Blangy, A., 2009. The Rho GTPase Wrch1 regulates osteoclast precursor adhesion and migration. Int. J. Biochem. Cell Biol. 41, 1391–1401.
Borchers, A., Epperlein, H.H., Wedlich, D., 2000. An assay system to study migratory behavior of cranial neural crest cells in Xenopus. Dev. Genes Evol. 210, 217–222.
Broders-Bondon, F., Chesneau, A., Romero-Oliva, F., Mazabraud, A., Mayor, R., Thiery, J.P., 2007. Regulation of XSnail2 expression by Rho GTPases. Dev. Dyn. 236, 2555–2566.
Brown, M.C., West, K.A., Turner, C.E., 2002. Paxillin-dependent paxillin kinase linker and p21-activated kinase localization to focal adhesions involves a multistep activation pathway. Mol. Biol. Cell 13, 1550–1565.
Cheung, M., Chaboissier, M.C., Mynett, A., Hirst, E., Schedl, A., Briscoe, J., 2005. The transcriptional control of trunk neural crest induction, survival, and delamination. Dev. Cell 8, 179–192.
Chuang, Y.Y., Valster, A., Coniglio, S.J., Backer, J.M., Symons, M., 2007. The atypical Rho family GTPase Wrch-1 regulates focal adhesion formation and cell migration. J. Cell Sci. 120, 1927–1934.
Coles, E.G., Taneyhill, L.A., Bronner-Fraser, M., 2007. A critical role for Cadherin6B in regulating avian neural crest emigration. Dev. Biol. 312, 533–544.
Coniglio, S.J., Zavarella, S., Symons, M.H., 2008. Pak1 and Pak2 mediate tumor cell invasion through distinct signaling mechanisms. Mol. Cell. Biol. 28, 4162–4172.
de Amicis, F., Lanzino, M., Kisslinger, A., Cali, G., Chieffi, P., Ando, S., Mancini, F.P., Tramontano, D., 2006. Loss of proline-rich tyrosine kinase 2 function induces spreading and motility of epithelial prostate cells. J. Cell. Physiol. 209, 74–80.
De Calisto, J., Araya, C., Marchant, L., Riaz, C.F., Mayor, R., 2005. Essential role of non-canonical Wnt signalling in neural crest migration. Development 132, 2587–2597.
Deacon, S.W., Beeser, A., Fukui, J.A., Rennefahrt, U.E., Myers, C., Chernoff, J., Peterson, J.R., 2008. An isoform-selective, small-molecule inhibitor targets the autoregulatory mechanism of p21-activated kinase. Chem. Biol. 15, 322–331.
Essex, L.J., Mayor, R., Sargent, M.G., 1993. Expression of Xenopus snail in mesoderm and prospective neural fold ectoderm. Dev. Dyn. 198, 108–122.
Faure, S., Lee, M.A., Keller, T., ten Dijke, P., Whitman, M., 2000. Endogenous patterns of TGFbeta superfamily signaling during early Xenopus development. Development 127, 2917–2931.
Fuchs, S., Herzog, D., Sumara, G., Buchmann-Moller, S., Civenni, G., Wu, X., Chrostek-Grashoff, A., Suter, U., Ricci, R., Relvas, J.B., Brakebusch, C., Sommer, L., 2009. Stage-specific control of neural crest stem cell proliferation by the small rho GTPases Cdc42 and Rac1. Cell Stem Cell 4, 236–247.
Gao, Y., Dickerson, J.B., Guo, F., Zheng, J., Zheng, Y., 2004. Rational design and characterization of a Rac GTPase-specific small molecule inhibitor. Proc. Natl Acad. Sci. USA 101, 7618–7623.
Gauthier-Rouviere, C., Vignal, E., Meriane, M., Roux, P., Montcourier, P., Fort, P., 1998. RhoG GTPase controls a pathway that independently activates Rac1 and Cdc42Hs. Mol. Biol. Cell 9, 1379–1394.
Groysman, M., Shoval, I., Kalcheim, C., 2008. A negative modulatory role for rho and rho-associated kinase signaling in delamination of neural crest cells. Neural Dev. 3, 27.
Guemar, L., de Santa Barbara, P., Vignal, E., Maurel, B., Fort, P., Faure, S., 2007. The small GTPase RhoV is an essential regulator of neural crest induction in Xenopus. Dev. Biol. 310, 113–128.
Hamburger, V., Hamilton, H.L., 1992. A series of normal stages in the development of the chick embryo. 1951. Dev. Dyn. 195, 231–272.
Hopwood, N.D., Pluck, A., Gurdon, J.B., 1989. A Xenopus mRNA related to Drosophila twist is expressed in response to induction in the mesoderm and the neural crest. Cell 59, 893–903.
Huang, X., Saint-Jeannet, J.P., 2004. Induction of the neural crest and the opportunities of life on the edge. Dev. Biol. 275, 1–11.
Hwang, Y.S., Luo, T., Xu, Y., Sargent, T.D., 2009. Myosin-X is required for cranial neural crest cell migration in Xenopus laevis. Dev. Dyn. 238, 2522–2529.
Jaffe, A.B., Hall, A., 2005. Rho GTPases: biochemistry and biology. Annu. Rev. Cell Dev. Biol. 21, 247–269.

Kashef, J., Kohler, A., Kuriyama, S., Alfandari, D., Mayor, R., Wedlich, D., 2009. Cadherin-11 regulates protrusive activity in Xenopus cranial neural crest cells upstream of Trio and the small GTPases. Genes Dev. 23, 1393–1398.
Kellerer, S., Schreiner, S., Stolt, C.C., Scholz, S., Bosl, M.R., Wegner, M., 2006. Replacement of the Sox10 transcription factor by Sox8 reveals incomplete functional equivalence. Development 133, 2875–2886.
LaBonne, C., Bronner-Fraser, M., 1998. Neural crest induction in Xenopus: evidence for a two-signal model. Development 125, 2403–2414.
Le Douarin, N.M., Dupin, E., 2003. Multipotentiality of the neural crest. Curr. Opin. Genet. Dev. 13, 529–536.
Liu, J.P., Jessell, T.M., 1998. A role for rhoB in the delamination of neural crest cells from the dorsal neural tube. Development 125, 5055–5067.
Manabe, R., Kovalenko, M., Webb, D.J., Horwitz, A.R., 2002. GIT1 functions in a motile, multi-molecular signaling complex that regulates protrusive activity and cell migration. J. Cell Sci. 115, 1497–1510.
Matthews, H.K., Marchant, L., Carmona-Fontaine, C., Kuriyama, S., Larrain, J., Holt, M.R., Parsons, M., Mayor, R., 2008. Directional migration of neural crest cells in vivo is regulated by Syndecan-4/Rac1 and non-canonical Wnt signaling/RhoA. Development 135, 1771–1780.
Mayor, R., Morgan, R., Sargent, M.G., 1995. Induction of the prospective neural crest of Xenopus. Development 121, 767–777.
Nagoshi, N., Shibata, S., Nakamura, M., Matsuzaki, Y., Toyama, Y., Okano, H., 2009. Neural crest-derived stem cells display a wide variety of characteristics. J. Cell. Biochem. 107, 1046–1052.
Nie, S., Kee, Y., Bronner-Fraser, M., 2009. Myosin-X is critical for migratory ability of Xenopus cranial neural crest cells. Dev. Biol. 335, 132–142.
Nieuwkoop, P.D., Faber, J., 1967. In: Daudin (Ed.), Normal Table of Xenopus laevis. Amsterdam, North-Holland.
Notarnicola, C., Le Guen, L., Fort, P., de Santa Barbara, P., 2008. Dynamic expression patterns of RhoV/Chp and RhoU/Wrch during chicken embryonic development. Dev. Dyn. 237, 1165–1171.
Ory, S., Brazier, H., Blangy, A., 2007. Identification of a bipartite focal adhesion localization signal in RhoU/Wrch-1, a Rho family GTPase that regulates cell adhesion and migration. Biol. Cell 99, 701–716.
Petrie, R.J., Doyle, A.D., Yamada, K.M., 2009. Random versus directionally persistent cell migration. Nat. Rev. Mol. Cell Biol. 10, 538–549.
Rangarajan, J., Luo, T., Sargent, T.D., 2006. PCNS: a novel protocadherin required for cranial neural crest migration and somite morphogenesis in Xenopus. Dev. Biol. 295, 206–218.
R Development Core Team, 2004. R: A Language and Environment for Statistical Computing. R Foundation for Statistical Computing, Vienna (Austria).
Ridley, A.J., Schwartz, M.A., Burridge, K., Firtel, R.A., Ginsberg, M.H., Borisy, G., Parsons, J.T., Horwitz, A.R., 2003. Cell migration: integrating signals from front to back. Science 302, 1704–1709.
Robertson, S.H., Smith, C.K., Langhans, A.L., McLinden, S.E., Oberhardt, M.A., Jakab, K.R., Dzamba, B., DeSimone, D.W., Papin, J.A., Peirce, S.M., 2007. Multiscale computational analysis of Xenopus laevis morphogenesis reveals key insights of systems-level behavior. BMC Syst. Biol. 1, 46.
Rupp, P.A., Kulesa, P.M., 2007. A role for RhoA in the two-phase migratory pattern of post-otic neural crest cells. Dev. Biol. 311, 159–171.
Ruusala, A., Aspenstrom, P., 2008. The atypical Rho GTPase Wrch1 collaborates with the nonreceptor tyrosine kinases Pyk2 and Src in regulating cytoskeletal dynamics. Mol. Cell. Biol. 28, 1802–1814.
Sadaghiani, B., Thiebaud, C.H., 1987. Neural crest development in the Xenopus laevis embryo, studied by interspecific transplantation and scanning electron microscopy. Dev. Biol. 124, 91–110.
Saras, J., Wollberg, P., Aspenstrom, P., 2004. Wrch1 is a GTPase-deficient Cdc42-like protein with unusual binding characteristics and cellular effects. Exp. Cell Res. 299, 356–369.
Sauka-Spengler, T., Bronner-Fraser, M., 2008. Evolution of the neural crest viewed from a gene regulatory perspective. Genesis 46, 673–682.
Schiavone, D., Dewilde, S., Vallania, F., Turkson, J., Di Cunto, F., Poli, V., 2009. The RhoU/Wrch1 Rho GTPase gene is a common transcriptional target of both the gp130/STAT3 and Wnt-1 pathways. Biochem. J. 421, 283–292.
Schlessinger, K., Hall, A., Tolwinski, N., 2009. Wnt signaling pathways meet Rho GTPases. Genes Dev. 23, 265–277.
Shutes, A., Berzat, A.C., Chenette, E.J., Cox, A.D., Der, C.J., 2006. Biochemical analyses of the Wrch atypical Rho family GTPases. Methods Enzymol. 406, 11–26.
Spokony, R.F., Aoki, Y., Saint-Germain, N., Magner-Fink, E., Saint-Jeannet, J.P., 2002. The transcription factor Sox9 is required for cranial neural crest development in Xenopus. Development 129, 421–432.
Symons, M., 2000. Adhesion signaling: PAK meets Rac on solid ground. Curr. Biol. 10, R535–R537.
Tao, W., Pennica, D., Xu, L., Kalejta, R.F., Levine, A.J., 2001. Wrch-1, a novel member of the Rho gene family that is regulated by Wnt-1. Genes Dev. 15, 1796–1807.
Thiery, J.P., Acloque, H., Huang, R.Y.J., Nieto, M.A., 2009. Epithelial–mesenchymal transitions in development and disease. Cell 139, 871–890.
Vignal, E., De Toledo, M., Comunale, F., Ladopoulou, A., Gauthier-Rouviere, C., Blangy, A., Fort, P., 2000. Characterization of TCL, a new GTPase of the rho family related to TC10 andCcdc42. J. Biol. Chem. 275, 36457–36464.
Vignal, E., de Santa Barbara, P., Guemar, L., Donnay, J.M., Fort, P., Faure, S., 2007. Expression of RhoB in the developing Xenopus laevis embryo. Gene Expr. Patterns 7, 282–288.
Weisz Hubsman, M., Volinsky, N., Manser, E., Yablonski, D., Aronheim, A., 2007. Autophosphorylation-dependent degradation of Pak1, triggered by the Rho-family GTPase, Chp. Biochem. J. 404, 487–497.
Wu, C.F., Delsert, C., Faure, S., Traverso, E.E., Kloc, M., Kuang, J., Etkin, L.D., Morin, N., 2007. Tumorhead distribution to cytoplasmic membrane of neural plate cells is positively regulated by Xenopus p21-activated kinase 1 (X-PAK1). Dev. Biol. 308, 169–186.
Wu, X., Tu, X., Joeng, K.S., Hilton, M.J., Williams, D.A., Long, F., 2008. Rac1 activation controls nuclear localization of beta-catenin during canonical Wnt signaling. Cell 133, 340–353.
Zhao, Z.S., Manser, E., Loo, T.H., Lim, L., 2000. Coupling of PAK-interacting exchange factor PIX to GIT1 promotes focal complex disassembly. Mol. Cell. Biol. 20, 6354–6363.